ELSEVIER

HIGHLIGHTED PAPER

RESEARCH: REVIEW

Mechanistic insight into the impact of pre-lithiation on the cycling stability of lithium-ion battery

Jinran Sun [1,2,#], Lang Huang [1,#], Gaojie Xu [1], Shamu Dong [1,*], Chunsheng Wang [3,4,*], Guanglei Cui [1,2,*]

[1] Qingdao Industrial Energy Storage Research Institute, Qingdao Institute of Bioenergy and Bioprocess Technology, Chinese Academy of Sciences, Qingdao 266101, China
[2] Center of Materials Science and Optoelectronics Engineering, University of Chinese Academy of Sciences, Beijing 100049, China
[3] Department of Chemical and Biomolecular Engineering, University of Maryland College Park, MD 20740, USA
[4] Department of Chemistry and Biochemistry, University of Maryland College Park, MD 20740, USA

Pre-lithiation is critical for improving the energy density of lithium-ion batteries (LIBs) in practical applications. The pre-lithiation of the high-capacity anode with a large surface area enhances the initial coulombic efficiency (ICE) by compensating the lithium loss from the formation of solid electrolyte interphase (SEI). However, pre-lithiation also affects cycle life, which has been paid little attention to. Here, we first discuss the impact of pre-lithiation on the cycling stability of the full cells, which is closely related to anode material, the degree of pre-lithiation, and the stability of SEI. Then we provide suggestions on how to achieve both high energy density and long cycle life by pre-lithiation. The understanding of the correlation between pre-lithiation and cycling stability sheds light on achieving the optimal performance of lithium-ion batteries from pre-lithiation technology.

Keywords: Pre-lithiation; Cycling stability; Lithiation degree; Structural stability; Lithium loss

Introduction

Lithium-ion batteries have been widely used in consumer electronics and are penetrating to electric vehicles and large-scale renewable energy storage devices due to their well-balanced performance in energy density, cost, and life span [1–3]. In recent years, the ever-increasing "endurance mileage" anxiety stimulates the ever-growing demand for the high energy density of LIBs. A significant advance in electrode materials, as well as electrode processing, has significantly increased the cell energy density [4–6]. However, almost all the employed electrode materials are difficult to achieve their theoretical energy density values in practical battery systems, attributing to the inevitable active lithium loss occurring in the anode during cycling, especially in the initial charge/discharge cycle [7].

The loss of lithium in Li-ion batteries mainly includes two aspects: (I) the Li consumption due to the initial formation of solid electrolyte interface (SEI) on anodes. (II) the contact failure of lithiated materials and the reformation of SEI due to the severe volumetric variation during charge/discharge cycles. During the initial charge/discharge process, the parasitic reactions occurred between the electrode and electrolyte to form the SEI on the surface of the anode, which irreversibly consumes the lithium ions. The amount of active lithium consumed is closely related to the reactivity between electrode materials and electrolytes [8–11]. Generally, the more specific surface area exposed, the more consumption of the active lithium. In addition to the initial Li loss from SEI formation, alloy (Si and Sn [12]) and conversion type anode materials that experience a large volume expansion/shrinkage (>100%) during lithiation/delithiation also continuously consume Li. The increased internal stress leads to the crack of SEI and particle pulverization. And the SEI regenerated on fresh exposed surface not only consumes active lithium, but also

* Corresponding authors.
E-mail addresses: Dong, S. (dongsm@qibebt.ac.cn), Wang, C. (cswang@umd.edu), Cui, G. (cuigl@qibebt.ac.cn).
# These authors contributed equally to this work.

 https://doi.org/10.1016/j.mattod.2022.07.008

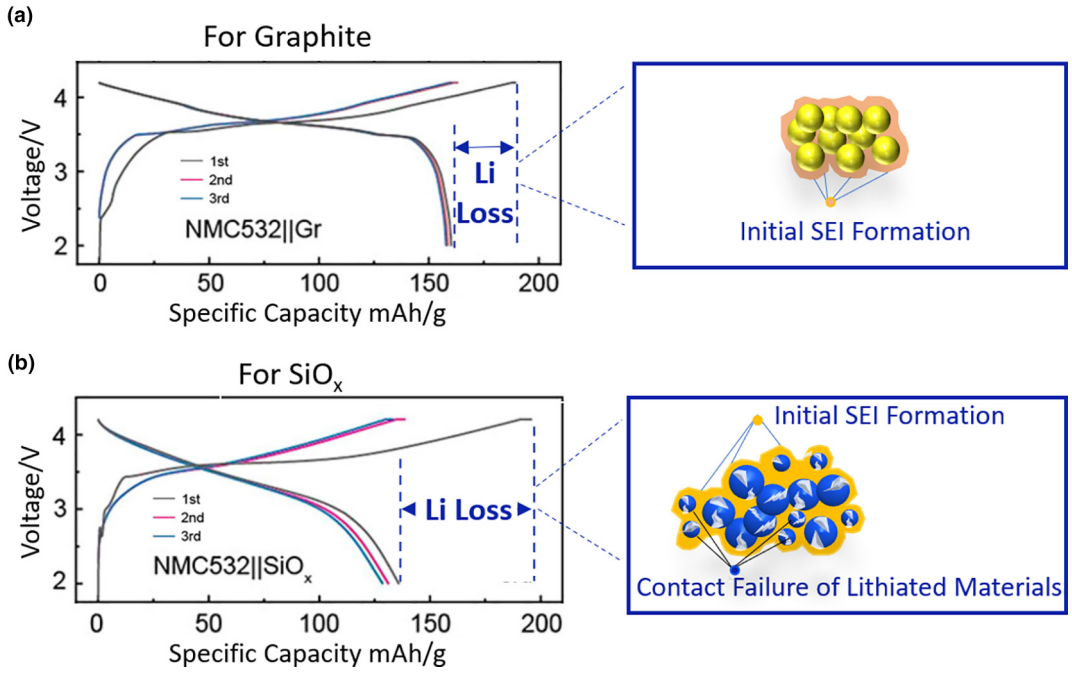

FIGURE 1

The initial charge–discharge curves of the full cells with different anodes and the corresponding schematic diagrams of initial lithium loss. (a) NMC532||Gr (b) NMC532||SiO_x [71]. Copyright 2021, The Royal Society of Chemistry.

isolates lithiated active materials from subsequent cycling (Fig. 1) [13,14]. All these factors lead to the decreased reversible capacity and the diminished energy density of the batteries.

Because of the inevitable lithium loss and the limited active lithium in the LIBs, pre-lithiation, which presets the extra Li sources to the electrode, is a prerequisite to obtain the improved initial coulombic efficiency and satisfactory energy density for the practical application of most LIBs. As the most promising technologies to promote the commercialization of the high energy density batteries, pre-lithiation strategy has been intensively investigated, which can be conducted by either electrochemically using half-cell, or chemically by directly contacting the anode with the lithium metal/pre-lithiation reagents prior to battery operation.[5,15–18].

Substantial reports have highlighted how the proposed pre-lithiation technologies improve ICE of the full cells, which represents the irreversible active lithium loss of the battery during the first cycle and is associated directly to the energy density of the cell. [19–27]. However, little attention has been paid to the influence of pre-lithiation on the cyclability. The pre-lithiation implemented in the full cells will certainly deepen the lithiation degree of the anode (even if it only compensates the active lithium loss in the initial cycling). The deeper lithiation degree will increase volume change, especially for alloy anodes, which poses a challenge to the stability of the SEI. Noting that the stability mentioned here is the structural integrity challenged by volume expansion, rather than the chemical stability affected by the components of SEI. The challenge would be pronounced for alloy/conversion type anode materials. In this case, pre-lithiation may lead to more lithium loss and the deterioration of cycling performance. However, if the fracture toughness of SEI is high enough to accommodate the volume variation, properly increasing the amount pre-lithiation (below the point that leads to lithium plating) can create an additional lithium inventory, improving the cycling performance by compensating the lithium loss during the cycling. As discussed above, the correlation between pre-lithiation and cycling stability of the full cell is intricate. This is a universal issue inevitably involved, which is often overlooked in academic literature. Clarifying this issue and its corresponding mechanism is of great significance for guiding practical industrial production.

Herein, by analyzing the published reports and our recent findings, we established the correlation between the cycling stability and the pre-lithiation in full cells, as illustrated in Fig. 2. The underpinning mechanism determined by the lithiation degree and the SEI stability was discussed in detail. Moreover, we recommended the rational design and processing for pre-lithiation to achieve the optimal performance of the lithium-ion batteries.

The intricate impacts of pre-lithiation on cycling stability

The impacts of pre-lithiation on cycling stability can be classified into three circumstances based on the volume change of the anodes: (1) positive impact for the anodes with small volume variation (such as graphite and hard carbon materials); (2) the unpredictable impact for the alloy/conversion type anodes; (3) the complicated impact for SiO/Si/graphite composites. The interactional lithium distribution between silicon and carbon after pre-lithiation impacts the cycling performance. Each part discusses corresponding mechanism underpinning the cyclability variation combining with typical example.

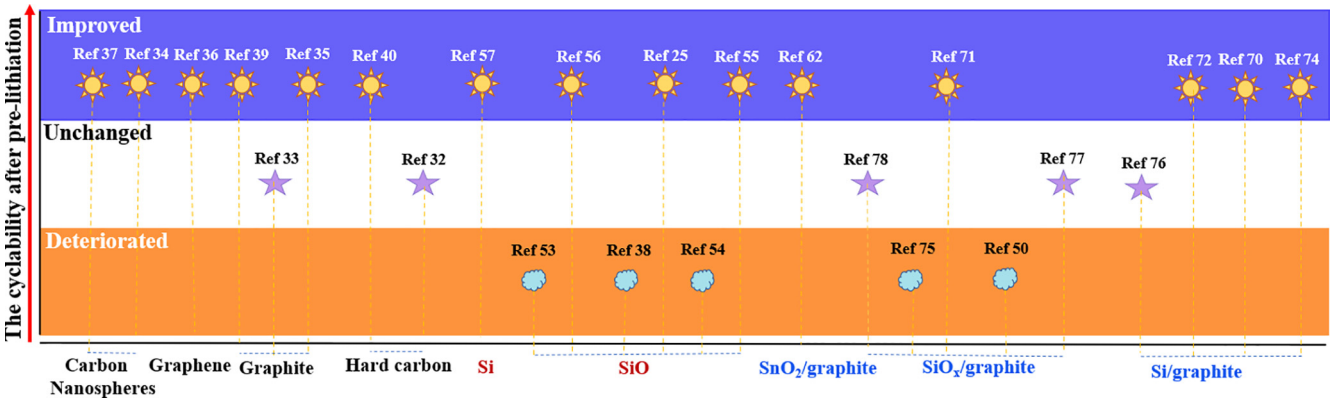

FIGURE 2

The statistical diagram of the cycling performance variations after pre-lithiation (full cells with different anodes). Different color blocks represent the cyclability variation of the pre-lithiated full cells compared to that without pre-lithiation: yellow-deteriorated, white-unchanged, purple-improved.

Carbon materials

The primary reason for the active lithium loss in carbon materials (such as graphite, hard carbon) is the formation of organic–inorganic SEI in the initial few charge/discharge cycles. The SEI strongly bonded to carbon can accommodate the <20% of volume changes during lithiation/delithiation of carbon anodes, achieving a long cycle life [28–31]. Because the stress incurred by the pre-lithiation is little, the pre-lithiated anode as well as SEI can well maintain structural integrity, without causing extra lithium loss. For the anode with low degree of pre-lithiation, the pre-loaded lithium is only used to compensate the active lithium loss related to the initial formation of the SEI during the first cycle. The cyclability of the full cell after pre-lithiation is almost unchanged compared with the one without pre-lithiation (Fig. 3a) [32,33]. However, for anodes with the high degree of pre-lithiation, the pre-loaded lithium can exist as a lithium inventory in the anode after compensating the active lithium loss in the first cycle, which will constantly replenish the active lithium loss during cycling until exhausted. Therefore, the pre-lithiation will improve the cycling stability of the full cells (Fig. 3b) [34–40].

Suggestion for pre-lithiation: reasonably increasing the degree of lithiation. After compensating the initial capacity loss for the formation of SEI, the additional amount lithium from pre-lithiation can serve as the lithium inventory, which can replenish the active lithium loss during cycling for a longer term. Thus, enhanced cycling performances can be achieved. However, if the total amount of lithium in the pre-lithiated full cell exceeds the capacity of anode, the lithium plating on the anode will occur, generating lithium dendrite, inducing severe active lithium loss and safety concerns. To achieve a reasonable amount of pre-lithiation, the principle can be described as follows:

$$\text{The amount of pre - loaded lithium} \leqslant A_{half} - C_{full}.$$

A_{half} is the lithiation capacity of the anode which obtained in the anode-Li half-cell, and C_{full} is the initial delithiation (discharge) capacity that obtained in the practical full cell. In addition to electrochemical testing, the lithiation degree of the anode can be accurately determined by the quantitative analysis of lithiation products, via solid state nuclear magnetic resonance (NMR). And the on-line gas analysis mass spectrometry system can be used as an auxiliary method to detect the content of inactive Li in cycled electrode through monitoring the evolution of H_2 during water titration, judging the impact of the pre-loaded lithium [41,42].

Alloy and conversion type anodes

Different from the carbon materials, the alloy and conversion type anodes always suffer from huge volume deformation during lithiation and de-lithiation [43–45]. Take Si as an example, the lithiation induced volume variation of the Si anode is nonlinear and drastic [28,46]. In the initial process, the lithium ions are inserted into the interstitial sites of Si to form amorphous Li_xSi. The Si electrode experiences elastic and plastic volume expansion, which can be partially accommodated by the electrode porosity. Upon further lithiation, the second phase reaction occurs. The abrupt appearance of $Li_{15}Si_4$ induces the rearrangement of Si structure. At the same time, the volume expands steeply. The rapidly increased internal stress greatly threatens the structural stability of SEI, which may lead to irreversible loss of electrolyte and lithiated materials [47]. Furthermore, as reported, for Si anode, the volume variation rate of the de-lithiation is more rapid than that of lithiation [28]. In this process, the steep volume contraction can easily result in the breakage of Si particles and create more electrically disconnected Si nanoparticles, causing significant decay of the capacity [48,49]. Most of the conclusions are also applicable to SiO_x, which is composed of Si domains and the SiO_x matrix [8,45,50].

Pre-lithiation improves the ICE of the full cells, and inevitably deepens the lithiation degree of in the lithiated anode meanwhile, which means more $Li_{15}Si_4$ will be formed (Fig. 4). The increased amount of $Li_{15}Si_4$ severely challenges the structural stability of the SEI and the subsequent cycling stability especially in the Si anode with the particle diameter over 150 nm, where the stored strain energy from electrochemical reactions and the relatively inhomogeneous lithiation will build up of large tensile hoop stress on the surface of the particles [51,52]. If the SEI fracture toughness cannot withstand the stress induced by the increased $Li_{15}Si_4$, the lithium loss caused by the SEI reformation and contact failure of lithiated materials will increase (Fig. 5a). In the subsequent cycle, the lithiation degree of pre-lithiated anode is deeper than that of anode without pre-lithiation due to the

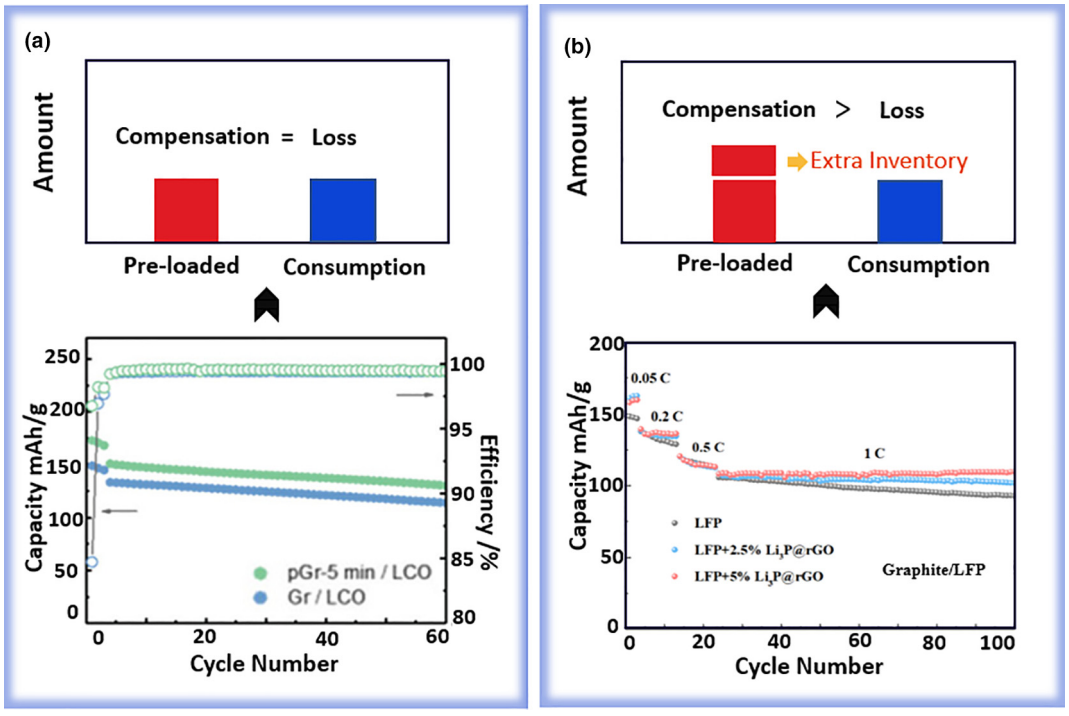

FIGURE 3

The schematic diagram of trade-off in the pre-lithiated full cells and the corresponding reported data (intercalation anodes). (a) Cycling performance and Coulombic efficiency of full cells with LCO as cathodes and Gr (pristine graphite) and pGr-5 min (pre-lithiated graphite) as the anode [33]. The cyclability of the full cells after pre-lithiation has no obvious change. Copyright 2021, WILEY-VCH (b) Electrochemical properties of LFP//graphite full cell with and without the Li_3P@rGO composite [36]. Because of the extra lithium inventory, the cyclability of the full cells after pre-lithiation is significantly improved. Copyright 2021, American Chemical Society.

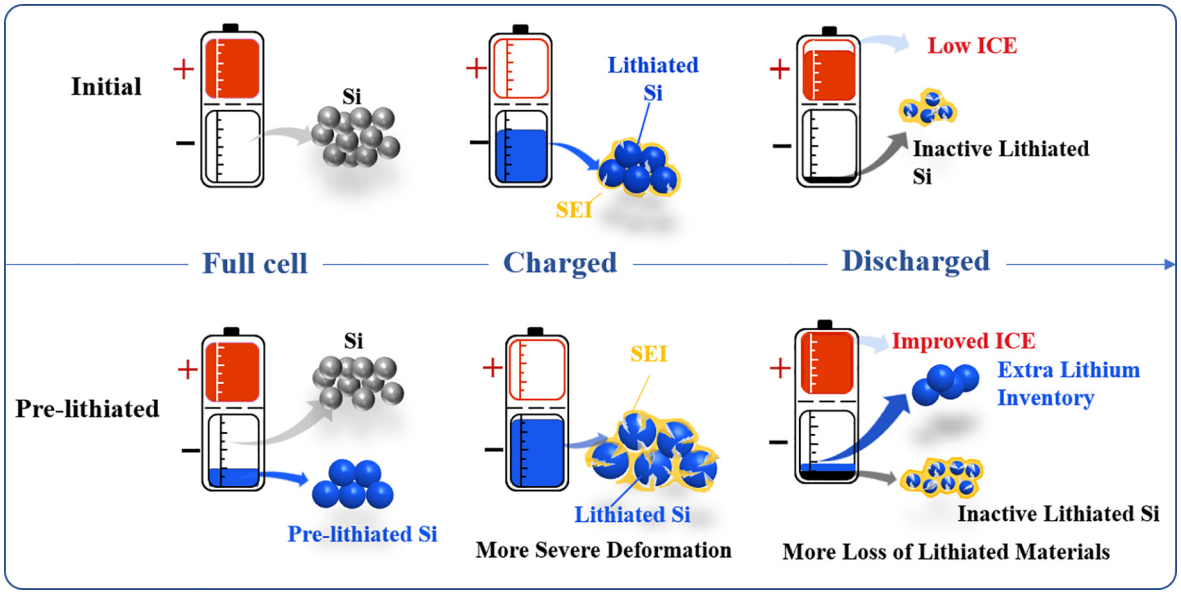

FIGURE 4

The schematic of the active lithium loss in the initial full cell with silicon anode and the pre-lithiated full cell with silicon anode. The red blocks and blue blocks represent the reversible capacity in the cathode and anode, respectively. The white blocks and the black blocks represent the un-lithiated active material and the inactive lithiated material, respectively.

loss of active material occurring in the first cycle, leading to deteriorated cycling performance (as summarized in Fig. 2). As shown in Fig. 6a, the pre-lithiated SiO_x/NCA full cell shows obviously deteriorated cycling stability, and the capacity retention after 100 cycles decreases from 76.97% to 61% [53]. The same situation also has been reported in other systems, such as the pre-lithiated SiO/NMC622 full cells [54]. It should be noted that most of the pre-lithiated cells mentioned above did not maxi-

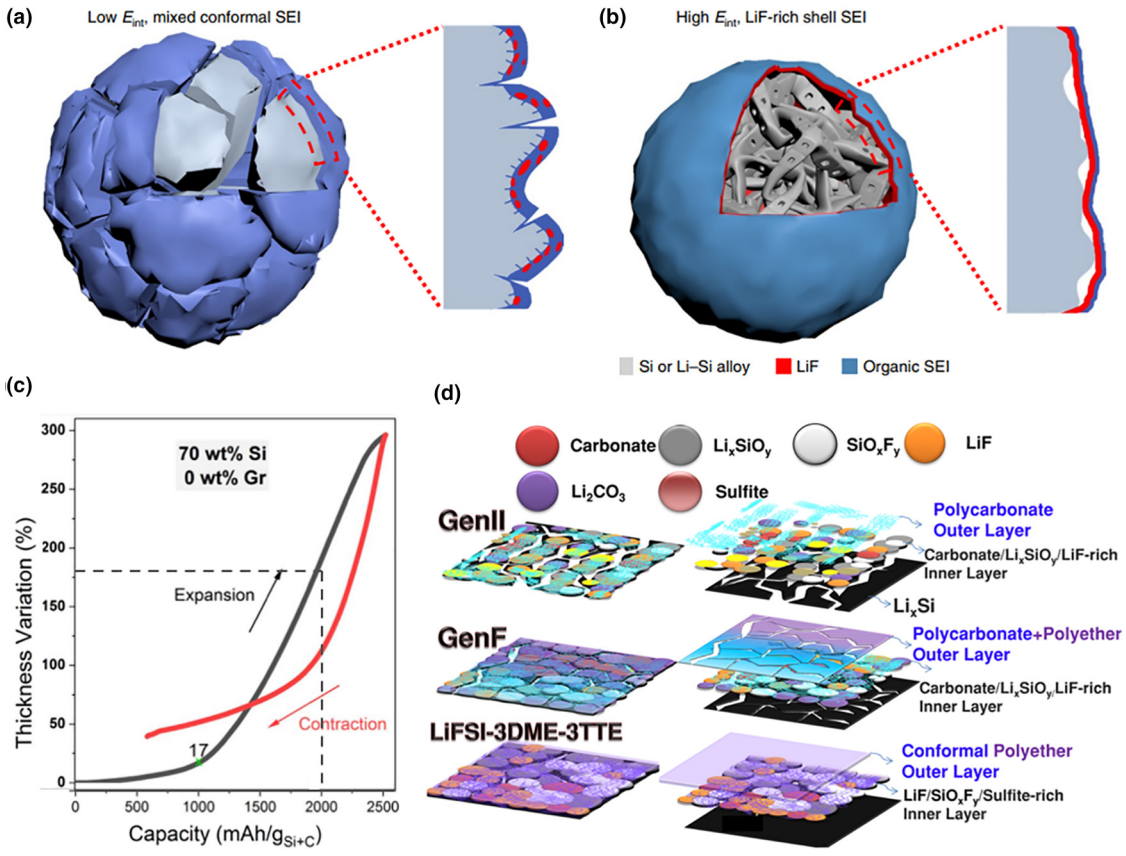

FIGURE 5

Schematic of the cycled alloy anode with an organic, low E_{int} and non-uniform (a) and an inorganic, high E_{int} and uniform (b) Li alloy–SEI interface [58]. Copyright 2020, Springer Nature (c) Thickness variation vs specific capacity for the third cycle of the 70 wt% Si electrodes. The anode expansion during the lithiation is displayed in black, while the electrode contraction curves during de-lithiation is represented in red [28]. Copyright 2020, American Chemical Society (d) Illustrations of the composite (left) and partitioned (right) views of the SEIs formed in CarEls (carbonate-based electrolytes) and GlyEl (glyme-based electrolytes) after extended cycling [64]. Copyright 2021, American Chemical Society.

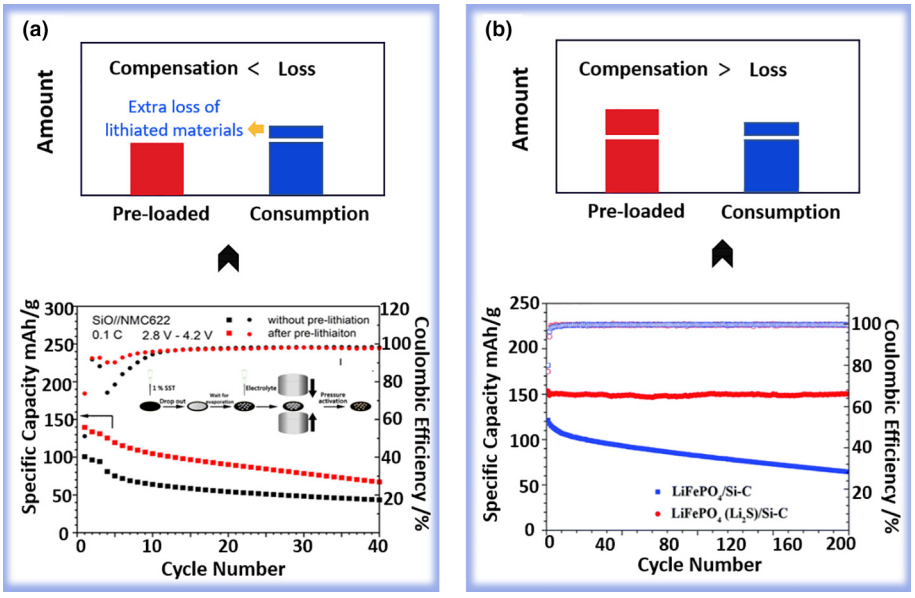

FIGURE 6

The schematic diagram of the cycling stability changes after pre-lithiation and the corresponding reported data (silicon-based anodes). (a) Capacity retention and coulombic efficiency of the SiO/NMC 622 [54]. The cyclability of the full cells after pre-lithiation is deteriorated. Copyright 2021, American Chemical Society (b) Capacity retention and coulombic efficiency of the $LiFePO_4$/Si–C and the $LiFePO_4$ (Li_2S)/Si–C full cells [65]. The cyclability of the full cells after pre-lithiation is significantly improved. Copyright 2018, The Royal Society of Chemistry.

mize the initial discharge capacity, indicating that the pre-loaded lithium only compensates the lithium loss during the initial cycle. There is no additional lithium inventory in these anodes. Even additional lithium inventory is introduced into the anode by increasing the amount of pre-loaded lithium, the competition between the lithium loss (due to deeper lithiation degree) and the lithium compensation (additional lithium inventory) will make the cycling stability (after pre-lithiation) unpredictable, as the lithium inventory would create more active lithium loss at the same time [38,55,56].

Whereas, if the SEI on the anode can maintain the structural integrity when facing increased stress caused by the deeper lithiation degree, the cycling stability of the full cells after pre-lithiation can be significantly improved. According to the report by Qian et al., the pre-lithiated anode(Si@Li_2SiO_3) can exhibit improved cycling stability compared with that of the anode without pre-lithiation (capacity retention increased from 41% to 83.6%) due to the Li_2SiO_3 layer which can strengthen the integrity of the electrode [57]. Recent study also provides a new pathway to achieve this point by fabricating a LiF-rich SEI with a high interface energy against Li via the design of the electrolyte (Fig. 5b), which can accommodate deformation of the alloy and effectively decrease the lithium loss [58]. In the $LiPF_6$-mixTHF electrolyte (2.0 M LiPF6 in a 1:1 v/v mixture of tetrahydrofuran and 2-methyltetrahydrofuran), the high degree of $LiPF_6$ association pushed the onset of the its reduction potential, enabling the formation of high-purity LiF inner SEI layer. Because LiF has high E_{int} (interfacial energy) with lithium silicate and Li_xSi, the Li_xSi can relocate at the inner layer of SEI to well accommodate the volume deformation. Thus, the SEI deformation and rupture during the alloy expansion can be effectively suppressed. Correspondingly, numerous electrolyte additives have been developed for improving the robustness of the SEI, particularly the additives that can decompose to fluorine-rich species. Fluoroethylene carbonate (FEC), which has been proved as an effective electrolyte additive for the electrolyte in the cells with silicon, can form a kinetically stable SEI comprising predominately lithium fluoride and lithium oxide and greatly stabilize the interface on anode [59]. Besides, designing the electrode structure rationally can alleviate the stress on SEI to some extent, solving the issue of the SEI fracture induced by the severe volume variation especially in the deeper lithiation degree, decreasing the active lithium loss, for instance, the Si microparticle encapsulated with the conformal graphene cage as well as the watermelon-inspired Si/C microspheres [60,61]. In short, for the anode materials with large volume variation during lithiation/de-lithiation, the cyclability evolution trend after pre-lithiation is associated directly with the degree of the pre-lithiation and the structural stability of SEI. Inappropriate application of pre-lithiation even deteriorates the cycling performance of the full cells. In addition to the silicon mentioned above, other anode materials (such as Sn, SnO_2) with huge volume deformation also face the same issue [62,63].

Suggestions for pre-lithiation:

(1) Properly adjusting the N/P ratio and the lithiation degree at the same time. When the full cell using Si anode is charged, smaller N/P ratio leads to deeper lithiation of the anode, and more $Li_{15}Si_4$ formation after pre-lithiation. A higher N/P ratio can reduce the lithiation degree of the anode, and appropriately increasing the amount of pre-loaded lithium can create extra lithium inventory in anode. According to the volume variation profiles *vs* specific capacity, controlling the lithiation state of the silicon anode under the specific capacity of 2000 mAh/g can significantly reduce volume variation (Fig. 5c), compared with that of the fully lithiated silicon anode [28]. The depletion rate of lithium inventory can be greatly decreased and the pre-lithiation can promote better cycling stability.

(2) Optimizing the components and structure of SEI. The optimization of SEI involves a comprehensive consideration of the factors at the interface, namely the active material of silicon particles, the binders, and the electrolytes. Among them, the design of electrolyte should be highlighted, which is crucial for achieving a favorable SEI with enhanced fracture toughness. Several enhanced SEI based on smart electrolyte design, such as elastic polyether enriched SEI reported by Nanda et al.(Fig. 5d) [64], LiF-based SEI from Chen et al. [58], can maintain the integrity of structure upon cycling and effectively improve the cycling stability of Si anode. The improved structural stability of SEI can protect Si from severe fracturing, avoiding the issues caused by active lithium loss.

Composite anodes

Si (SiO_x)-graphite is one of the most widely used composite anode materials in the modern industry [66], and pre-lithiation is essential for these materials to achieve higher energy density. Except the volume variation caused by the deeper lithiation, the lithium distribution in the lithiated anode also presents a significant influence on the cycling stability. The trade-off between the lithium compensation and consumption after pre-lithiation is more complicated in this composite system, because the lithiation potential of graphite is close to the $Li_{15}Si_4$ formation potential (around 90–100 mV) [67], as illustrated in our recent finding [68]. Through solid state NMR, we traced the evolution of active lithium distribution in the lithiated SiO_x-graphite composite anode before/after pre-lithiation (taken out from the fully charged full cells). Compared with the anode without pre-lithiation, the proportion of LiC_x and $Li_{15}Si_4$ have notably increased in the pre-lithiated anode simultaneously. The additional lithium storage in LiC_x is favorable for long cycle lifespan due to the excellent reversibility of graphite. However, as discussed above, $Li_{15}Si_4$ is the major source for electrode deformation, which results in the fracture of the SEI and contact failure of active materials. In this case, the lithium distributed at $Li_{15}Si_4$ poses a challenge for the overall cycling performance [69].

The unfavorable lithium distribution at $Li_{15}Si_4$ in the composite anode triggers intricate impacts on the cycling performance of the pre-lithiated full cells. The cycling stability of the full cells with composite anodes displays various trends (improved (Fig. 6b) [65,70–74], deteriorated [50,75], and unchanged [76–78]). Besides the stability of SEI, the cyclability of the pre-lithiated composite anode is also closely associated with the

degree of the pre-lithiation, and the composition and proportion of the anodes.

Suggestions for pre-lithiation of composite anodes:

Improving the cyclability of the pre-lithiated composite anodes makes a great significance for its practical large-scale application. In addition to the aforementioned strategies for the optimization of the pre-lithiated silicon anodes [60,79–85], there are some proposals specifically aimed at realizing the optimized cycling stability of the composite anode:

(1) The adjustment of the composition proportion. The key point is to increase the amount of pre-loaded as an inventory. To prevent lithium plating, the specific capacity of anode should be improved along with the N/P ratio. If the proportion of silicon or SiO is appropriately increased with the enlarged N/P ratio, the lithiation degree of the anode will be decreased, which can reduce volume deformation of silicon. Thus, the pre-lithiated full cells with improved cycling stability can be achieved owing to the decreased active lithium loss and the contribution of increased lithium inventory.

(2) Separating the lithiation potential. Developing effective methods to separate the lithiation potential of LiC_x and $Li_{15}Si_4$. Improving the utilization rate of highly reversible graphite and reducing the amount of $Li_{15}Si_4$ are of great significance for optimizing the cyclability of the composite anode.

We proposed a LiF induced selective lithiation strategy to separate the formation potential of LiC_x and $Li_{15}Si_4$ (Fig. 7). Due to the difference of interface separation energy (W_{sep}, the ideal work of separation, which models the required energy of idealized separation of the interface into two surfaces in vacuum [86]) between LiF and the active materials (Si, SiO, and graphite), LiF can in-situ preferentially accumulate on local $Si@SiO_x$ particles. The LiF with poor ionic and electronic conductivity slows down the lithiation kinetic at $Si@SiO_x$ particles and makes the $Li_{15}Si_4$ form at lower potential, significantly improving the utilization rate of graphite and reducing the amount of $Li_{15}Si_4$. As a result, the cycling stability of the pre-lithiated $Si@SiO_x/C$ composite anode is significantly improved through unshackling the highly reversible lithium storage capability of graphite from the redundancy capacity. In an ultra-high area capacity (NCA/S450, 4.9 mAh/cm^2) full cell demonstration, the capacity retention can be significantly improved from 85% to 94.2% after 300 cycles.

Outlook and conclusions

Attention should be paid to the by-products or the residues generated by the pre-lithiation reagents, which may have certain impacts on cycling stability through changing the composition or structure of SEI. For example, the implement of some chemical pre-lithiation which required the electrode to be immersed in a specific pre-lithiation solution, generally faces the issue of residual organic reagents, because it is difficult to clean thoroughly, which may affect the formation and the chemical stability of SEI. Even the incompletely decomposed reagents and the by-products are inert, such as the byproduct (N_2) from Li_3N, it also poses impacts on internal environment and the energy density of the battery, which should be taken into account for the industrial applications [87]. Moreover, attention should be paid to the safety hazards of ex-situ pre-lithiation, such as the heat release during pre-lithiation and the environmental stability of the material (lithium foil, lithium powder). By contrast, the in-situ pre-lithiation technologies without introducing inactive elements and damaging electrode structure should be a promising approach. For instance, as reported by Suo et al. $Li_2[Ni_{0.8}Co_{0.1}Mn_{0.1}]O_2$ can act as a Li-ions extender to release a large amount of Li-ions during the first charging process then convert into NCM811, thus supplementing the Li loss without the introduction of inactive elements [88].

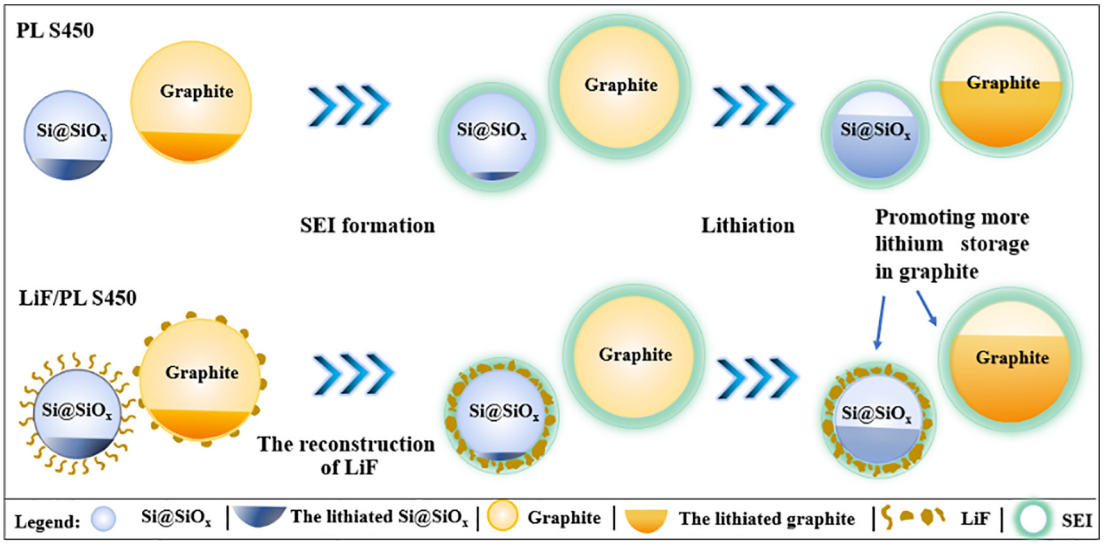

FIGURE 7

The illustration of SEI formation and the lithiation state of different anodes. PL S450: pre-lithiated S450 anode; LiF/PL S450: pre-lithiated S450 anode modified by LiF. From left to right, the original state of the anodes, the state of the anodes after they are immersed in the electrolyte, and the lithiated state of the anodes. The grey circle and the blue circle represent the state of graphite and the $Si@SiO_x$ in different anodes, respectively.

Multifunctional pre-lithiation technologies are highly desirable. For instance, the mixture of Li_2O and MgO can serve as an effective pre-lithiation reagents for the industrial level preparation of SiO. The reaction products, $Li_xMg_ySi_zO_n$, can stabilize SEI structure and improve the transport efficiency of lithium ion in SEI [89]. The Li_3P, with a high Li content of 57.82 mol_{Li}/kg, has been applied to compensate for the active lithium loss. After the initial extraction of Li^+, the residual phosphorus remaining on the cathode can work as a fire retardant, improving the energy density and safety of the full cell at the same time [36]. In addition to the optimization of pre-lithiation reagents, the processes can also be adjusted to achieve multifunctional pre-lithiation. A case in point is the recently reported lithium-biphenyl pre-lithiation method. Because of the homogeneous Li organic complex pre-lithiation solution and high-temperature calcination process, it introduces extra lithium as well as improves the structural integrity of the electrode, decreasing the irreversible active material loss upon cycles [90]. Besides, the direct formation of high quality SEI through pre-lithiation to reduce the consumption of electrolyte during battery operation is a promising method in industrial applications, which has been rarely reported and the extensive exploration is required.

In summary, pre-lithiation is a widely applied technology to improve the energy density of lithium-ion batteries by providing additional lithium to compensate the lithium loss. It is worth pointing out that the pre-lithiation has a complicated effect on the cycling stability of the lithium-ion batteries, which is closely related to the degree of pre-lithiation and the stability of SEI. The mechanism underpinning the cyclability variation after pre-lithiation is elucidated building upon the systematically summarizing the existing reports. For the anodes with small volumetric deformations upon lithiation and de-lithiation, pre-lithiation usually has a positive effect on cycling stability. Nevertheless, for materials such as silicon, tin, and the related composite anodes, while pre-lithiation replenishes the lithium loss, the inevitable deeper lithiation degree of the anode will severely challenge the structural stability of SEI. Inappropriate pre-lithiation may adversely affect the cycling stability of the full cells. It is of great significance to analyze the correlation and mechanism between cyclability and pre-lithiation in full cells with different kinds of anodes for guiding the application of pre-lithium technology in practical industrialization. The profound insights mentioned in this paper will provide beneficial guidance for pre-lithiation to achieve performance-enhanced lithium-ion battery in the future.

Declaration of Competing Interest

The authors declare that they have no known competing financial interests or personal relationships that could have appeared to influence the work reported in this paper.

Acknowledgments

This work is supported by the Strategic Priority Research Program of the Chinese Academy of Sciences (XDA21070304), the National Natural Science Foundation of China (22139001), Taishan Scholars Program for Young Expert of Shandong Province (No.tsqn 202103145), Shandong Energy Institute (SEI I202108), and Natural Science Foundation of Shandong Province (ZR2021QB030).

References

[1] R. Zhan et al., Adv. Energy Mater. 11 (2021) 2101565, https://doi.org/10.1002/aenm.202101565.
[2] X. Li et al., Nano Energy 77 (2020), https://doi.org/10.1016/j.nanoen.2020.105143 105143.
[3] M.N. Obrovac et al., J. Electrochem. Soc. 154 (2007) A849, https://doi.org/10.1149/1.2752985.
[4] R. Weber et al., Nat. Energy 4 (2019) 683–689, https://doi.org/10.1038/s41560-019-0428-9.
[5] F. Holtstiege et al., Batteries 4 (2018) 4, https://doi.org/10.3390/batteries4010004.
[6] F. Wang et al., Joule 2 (2018) 927–937, https://doi.org/10.1016/j.joule.2018.02.011.
[7] M.N. Obrovac, V.L. Chevrier, Chem. Rev. 114 (2014) 11444–11502, https://doi.org/10.1021/cr500207g.
[8] K. Kitada et al., J. Am. Chem. Soc. 141 (2019) 7014–7027, https://doi.org/10.1021/jacs.9b01589.
[9] X. Zhang, C. Fan, S. Han, J. Mater. Sci. 52 (2017) 10418–10430, https://doi.org/10.1007/s10853-017-1206-3.
[10] Y. Liu et al., Mater. Chem. Phys. 89 (2005) 80–84, https://doi.org/10.1016/j.matchemphys.2004.08.032.
[11] T. Chen et al., J. Power Sources 363 (2017) 126–144, https://doi.org/10.1016/j.jpowsour.2017.07.073.
[12] C. Li et al., Energy Environ. Mater. (2021), https://doi.org/10.1002/eem2.12267.
[13] K. Ogata et al., Nat. Commun. 5 (2014) 3217, https://doi.org/10.1038/ncomms4217.
[14] S. Li et al., Energy Storage Mater. 20 (2019) 7–13, https://doi.org/10.1016/j.ensm.2018.11.030.
[15] F. Wang et al., ACS Nano 15 (2021) 2197–2218, https://doi.org/10.1021/acsnano.0c10664.
[16] L. Jin et al., Adv. Sci. 8 (2021) e2005031.
[17] C.L. Berhaut et al., Energy Storage Mater. 29 (2020) 190–197, https://doi.org/10.1016/j.ensm.2020.04.008.
[18] H. Xu et al., Energy Environ. Sci. (2019), https://doi.org/10.1039/C9EE01404G.
[19] N. Liu et al., ACS Nano 5 (2011) 6487–6493, https://doi.org/10.1021/nn2017167.
[20] C.R. Jarvis et al., J. Power Sources 162 (2006) 800–802, https://doi.org/10.1016/j.jpowsour.2005.07.051.
[21] J.H. Yom et al., J. Electrochem. Soc. 165 (2018) A603–A608, https://doi.org/10.1149/2.0911803jes.
[22] J. Jang et al., Angew. Chem. 59 (2020) 14473–14480, https://doi.org/10.1002/anie.202002411.
[23] X. Li et al., Nat. Commun. 5 (2014) 4105, https://doi.org/10.1038/ncomms5105.
[24] H. Zhou, X. Wang, D. Chen, ChemSusChem 8 (2015) 2737–2744, https://doi.org/10.1002/cssc.201500287.
[25] G. Wang et al., Energy Storage Mater. 24 (2020) 147–152, https://doi.org/10.1016/j.ensm.2019.08.025.
[26] G. Wang et al., ACS Appl. Mater. Interfaces 11 (2019) 8699–8703, https://doi.org/10.1021/acsami.8b19416.
[27] X.L. Wang et al., J. Am. Chem. Soc. 133 (2011) 20692–20695, https://doi.org/10.1021/ja208880f.
[28] A.Y.R. Prado et al., J. Electrochem. Soc. 167 (2020), https://doi.org/10.1149/1945-7111/abd465 160551.
[29] P. Mohtat et al., J. Power Sources 427 (2019) 101–111, https://doi.org/10.1016/j.jpowsour.2019.03.104.
[30] S. Schweidler et al., J. Phys. Chem. C 122 (2018) 8829–8835, https://doi.org/10.1021/acs.jpcc.8b01873.
[31] A. Agrawal et al., J. Solid State Electrochem. 22 (2018) 3443–3455, https://doi.org/10.1007/s10008-018-4044-6.
[32] Y. Shen et al., Small 16 (2020) e1907602.
[33] Y. Shen et al., Adv. Funct. Mater. 31 (2021) 2101181, https://doi.org/10.1002/adfm.202101181.
[34] V.A. Sugiawati et al., Polymers 12 (2020), https://doi.org/10.3390/polym12020406.
[35] Z. Wang et al., J. Power Sources 260 (2014) 57–61, https://doi.org/10.1016/j.jpowsour.2014.02.112.
[36] X. Wang et al., ACS Appl. Energy Mater. 4 (2021) 5246–5254, https://doi.org/10.1021/acsaem.1c00773.

[37] F. Holtstiege et al., ACS Appl. Energy Mater. 1 (2018) 4321–4331, https://doi.org/10.1021/acsaem.8b00945.
[38] G. Ai et al., J. Power Sources 309 (2016) 33–41, https://doi.org/10.1016/j.jpowsour.2016.01.061.
[39] S.-Y. Yang et al., J. Power Sources 480 (2020), https://doi.org/10.1016/j.jpowsour.2020.229109 229109.
[40] X. Zhang et al., ACS Appl. Mater. Interfaces 12 (2020) 11589–11599, https://doi.org/10.1021/acsami.9b21417.
[41] D. Ren et al., eTransportation 2 (2019), https://doi.org/10.1016/j.etran.2019.100034.
[42] G. Xu et al., Angew. Chem. 60 (2021) 7770–7776, https://doi.org/10.1002/anie.202013812.
[43] T. Tan, P.-K. Lee, D.Y.W. Yu, J. Electrochem. Soc. 166 (2018) A5210–A5214, https://doi.org/10.1149/2.0321903jes.
[44] K. Pan et al., J. Power Sources 413 (2019) 20–28, https://doi.org/10.1016/j.jpowsour.2018.12.010.
[45] A. Hirata et al., Nat. Commun. 7 (2016) 11591, https://doi.org/10.1038/ncomms11591.
[46] X.H. Liu et al., Nat. Nanotechnol. 7 (2012) 749–756, https://doi.org/10.1038/nnano.2012.170.
[47] J.-H. Kim et al., J. Electroanal. Chem. 661 (2011) 245–249, https://doi.org/10.1016/j.jelechem.2011.08.010.
[48] Y. Reynier et al., J. Power Sources 450 (2020), https://doi.org/10.1016/j.jpowsour.2020.227699 227699.
[49] Y. Zhang et al., J. Energy Chem. 64 (2022) 615–650, https://doi.org/10.1016/j.jechem.2021.04.013.
[50] D.J. Chung et al., Nano Energy 89 (2021), https://doi.org/10.1016/j.nanoen.2021.106378 106378.
[51] X.H. Liu et al., ACS Nano 6 (2012) 1522–1531, https://doi.org/10.1021/nn204476h.
[52] P. Bärmann et al., J. Power Sources 464 (2020), https://doi.org/10.1016/j.jpowsour.2020.228224 228224.
[53] H.J. Kim et al., Nano Lett. 16 (2016) 282–288, https://doi.org/10.1021/acs.nanolett.5b03776.
[54] B. Huang et al., ACS Sustainable Chem. Eng. 9 (2021) 648–657, https://doi.org/10.1021/acssuschemeng.0c05851.
[55] L. Zhang et al., J. Power Sources 400 (2018) 549–555, https://doi.org/10.1016/j.jpowsour.2018.08.061.
[56] J. Zhao et al., PNAS 113 (2016) 7408–7413, https://doi.org/10.1073/pnas.1603810113.
[57] Y. Zhu et al., ACS Appl. Mater. Interfaces 11 (2019) 18305–18312, https://doi.org/10.1021/acsami.8b22507.
[58] J. Chen et al., Nat. Energy 5 (2020) 386–397, https://doi.org/10.1038/s41560-020-0601-1.
[59] K. Schroder et al., Chem. Mater. 27 (2015) 5531–5542, https://doi.org/10.1021/acs.chemmater.5b01627.
[60] Q. Xu et al., Adv. Energy Mater. 7 (2017) 1601481, https://doi.org/10.1002/aenm.201601481.
[61] Y. Li et al., Nat. Energy 1 (2016), https://doi.org/10.1038/nenergy.2015.29.
[62] F. Li et al., ACS Appl. Mater. Interfaces 12 (2020) 19423–19430, https://doi.org/10.1021/acsami.0c00729.
[63] H. Xu et al., Energy Environ. Sci. 12 (2019) 2991–3000, https://doi.org/10.1039/c9ee01404g.
[64] G. Yang et al., ACS Energy Lett. 6 (2021) 1684–1693, https://doi.org/10.1021/acsenergylett.0c02629.
[65] Y. Zhan et al., J. Mater. Chem. A 6 (2018) 6206–6211, https://doi.org/10.1039/c8ta00496j.
[66] X. Yang et al., Carbon 77 (2014) 275–280, https://doi.org/10.1016/j.carbon.2014.05.030.
[67] A. Tornheim, S.E. Trask, Z. Zhang, J. Electrochem. Soc. 166 (2019) A132–A134, https://doi.org/10.1149/2.0111902jes.
[68] Z.S. Sun et al., Sci. China Mater. (2022), https://doi.org/10.1007/s40843-021-2049-9.
[69] W.M. Dose et al., Chem. Commun. 54 (2018) 3586–3589, https://doi.org/10.1039/c8cc00456k.
[70] Z. Liu et al., ACS Appl. Mater. Interfaces 13 (2021) 11985–11994, https://doi.org/10.1021/acsami.0c22880.
[71] K.H. Kim et al., J. Power Sources 459 (2020), https://doi.org/10.1016/j.jpowsour.2020.228066 228066.
[72] J. Du et al., *Nano Lett.* 20 (2020) 546–552, https://doi.org/10.1021/acs.nanolett.9b04278.
[73] W.M. Dose et al., J. Electrochem. Soc. 167 (2020), https://doi.org/10.1149/1945-7111/abd1ef 160543.
[74] S. Abouali et al., 2D Materials 8 (2021), https://doi.org/10.1088/2053-1583/abe106.
[75] X. Zhang et al., J. Power Sources 478 (2020), https://doi.org/10.1016/j.jpowsour.2020.229067 229067.
[76] X. Liu et al., ACS Energy Lett. 6 (2020) 320–328, https://doi.org/10.1021/acsenergylett.0c02487.
[77] J. Choi et al., J. Am. Chem. Soc. 143 (2021) 9169–9176, https://doi.org/10.1021/jacs.1c03648.
[78] X. Liu et al., Nano Lett. 20 (2020) 4558–4565, https://doi.org/10.1021/acs.nanolett.0c01413.
[79] J. Zhao et al., J. Am. Chem. Soc. 137 (2015) 8372–8375, https://doi.org/10.1021/jacs.5b04526.
[80] M. Zhang et al., J. Alloy. Compd. 588 (2014) 206–211, https://doi.org/10.1016/j.jallcom.2013.10.160.
[81] Y. Son et al., Adv. Mater. 32 (2020) e2003286.
[82] B. Koo et al., Angew. Chem. 51 (2012) 8762–8767, https://doi.org/10.1002/anie.201201568.
[83] Y. Chen et al., J. Power Sources 298 (2015) 130–137, https://doi.org/10.1016/j.jpowsour.2015.08.058.
[84] Y. Hwa, C.-M. Park, H.-J. Sohn, J. Power Sources 222 (2013) 129–134, https://doi.org/10.1016/j.jpowsour.2012.08.060.
[85] S.S. Suh et al., Electrochim. Acta 148 (2014) 111–117, https://doi.org/10.1016/j.electacta.2014.08.104.
[86] N.D. Lepley, N.A.W. Holzwarth, Phys. Rev. B 92 (2015), https://doi.org/10.1103/PhysRevB.92.214201.
[87] K. Park, B.-C. Yu, J.B. Goodenough, Adv. Energy Mater. 6 (2016) 1502534, https://doi.org/10.1002/aenm.201502534.
[88] L. Lin et al., *Angew. Chem. Int. Ed.* 60 (2021) 8289–8296, https://doi.org/10.1002/anie.202017063.
[89] R.G. Singhal et al., J. Power Sources 128 (2004) 247–255, https://doi.org/10.1016/j.jpowsour.2003.09.064.
[90] M.Y. Yan et al., ACS Appl. Mater. Interfaces 12 (2020) 27202–27209, https://doi.org/10.1021/acsami.0c05153.